PERGAMON

International Journal of Solids and Structures 39 (2002) 341–350

INTERNATIONAL JOURNAL OF SOLIDS and STRUCTURES

www.elsevier.com/locate/ijsolstr

Some phenomena for lateral flutter of beams under follower load

F.M. Detinko

3098-G Whisper Lake Lane, Winter Park, FL 32792, USA

Received 10 March 2001; in revised form 12 August 2001

Abstract

Simple model of a slender beam loaded by a transverse follower force and undergoing a lateral flutter is used to demonstrate the following phenomena:

1. If an analysis does not include any damping, an extraction of only two lowest eigenvalues can lead to a wrong conclusion that the critical load is infinite. This is so because, when the ratio of two principal rigidities of a beam is not small, the eigenvalue with a positive real part emerges first not at the very beginning of the spectrum.
2. For the Kelvin-type material, and with no external damping, the critical load becomes infinitely small when the damping in the normal stress vanishes while the shear stress damping is finite.
3. When the external damping is increased, the critical load approaches the value calculated with no internal damping.

The nonlinear equilibrium is presented in the closed form and the eigenvalues of the torsional–flexural dynamic perturbed equations are found by the finite element approach and subdomain collocation method.

Keywords: Elastic; Stability; Flutter; Damping; Lateral

1. Introduction

The lateral stability of a beam under transverse follower force was analyzed first, apparently, by Bolotin (1963) for a pinned configuration and by Como (1966) for a cantilever beam.

The finite element formulation for the problem in question was given in Barsoum (1971). Some applications of the Barsoum (1971) formulation are given in Attard and Somervaille (1987). In all these works the prebuckling deformations and damping were ignored. For our purposes it is important also to emphasize that in Attard and Somervaille only two smallest eigenvalues were extracted to find a critical force. As will be shown below, this is justified only when the ratio of two principal rigidities of a beam is small.

E-mail address: felideti@magicnet.net (F.M. Detinko).

0020-7683/01/$ - see front matter
PII: S0020-7683(01)00202-5

In this paper the uniform beam under follower bending load is analyzed. The goal of this analysis is to estimate the effect of both internal and external damping on the critical load. It is also found that calculation of only two lowest eigenvalues is insufficient when the ratio of two principal rigidities of a beam is larger than 0.42. In this case the eigenvalue with a positive real part emerges first not at the beginning of the spectrum.

The nonlinear equilibrium state for an uniform beam is found in a closed form so that no iterations are needed. To analyze the stability of this equilibrium the eigenvalues of the perturbed equations of motion are calculated by the finite element approach in conjunction with the subdomain collocation method, as described in Detinko (2000). Using Mathcad 8 and 20 elements, all eigenvalues are easily extracted.

2. Equations of motion of an inextensional viscoelastic beam

For a slender beam the warping rigidity and the tension–torsion coupling may be neglected (see Hodges and Peters, 1975). Thus, the Kirchoff equations of motion for an initially straight beam, loaded by terminal forces, will be used.

In the coordinate system x_1, x_2, x_3 where x_1, x_2 are principal axes of the cross-section, Fig. 1, and x_3 is a tangent to the deformed axis of the beam, equations of motion are (see Love, 1944)

$$F_1' - \kappa_3 F_2 + \kappa_2 F_3 + J_1 = 0 \tag{1}$$

$$F_2' + \kappa_3 F_1 - \kappa_1 F_3 + J_2 = 0 \tag{2}$$

$$F_3' - \kappa_2 F_1 + \kappa_1 F_2 + J_3 = 0 \tag{3}$$

$$M_1' - \kappa_3 M_2 + \kappa_2 M_3 - F_2 = 0 \tag{4}$$

$$M_2' + \kappa_3 M_1 - \kappa_1 M_3 + F_1 = 0 \tag{5}$$

$$M_3' - \kappa_2 M_1 + \kappa_1 M_2 = 0 \tag{6}$$

Here

$$F = (F_1, F_2, F_3)^{\mathrm{T}}, \qquad M = (M_1, M_2, M_3)^{\mathrm{T}}, \qquad J = (J_1, J_2, J_3)^{\mathrm{T}}$$

is vector of internal force, moment, and inertia force, respectively. Components of curvature κ_1, κ_2 and twist κ_3 are expressed in terms of Euler angles θ, ϕ, ψ as

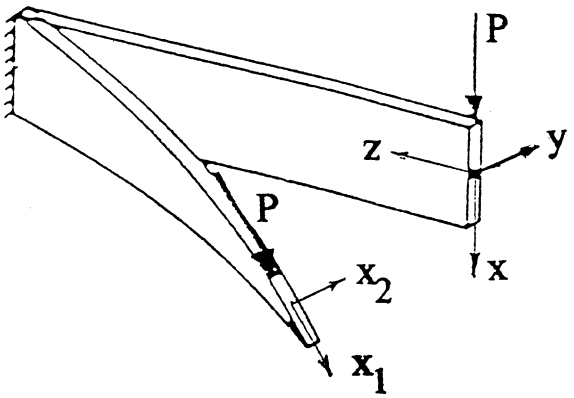

Fig. 1. Notations and loading.

$$\kappa_1 = \theta' \sin\phi - \psi' \sin\theta \cos\phi$$

$$\kappa_2 = \theta' \cos\phi + \psi' \sin\theta \sin\phi \tag{7}$$

$$\kappa_3 = \phi' + \psi' \cos\theta$$

Euler angles define the direction of the moving coordinate system x_1, x_2, x_3 with respect to fixed axes (x, y, z), and relations

$$x' = \sin\theta \cos\psi, \qquad y' = \sin\theta \sin\psi, \qquad z' = \cos\theta \tag{8}$$

hold. In Eqs. (1)–(8) and elsewhere a prime denotes the derivative with respect to the dimensionless arc of the deformed beam s/L. The forces, moments, and time are normalized by D_2/L^2, D_2/L, $\lambda = \sqrt{D_2/mL^4}$ respectively, where D_2 is the largest principal bending rigidity and m is the mass per unit of length. Vector of inertia force is

$$J = -H\ddot{X}, \quad X = (x, y, z)^{\mathrm{T}}$$

Elements of 3×3 matrix H are equal to

$$\begin{aligned} h_{11} &= -\sin\psi \sin\phi + \cos\psi \cos\phi \cos\theta, & h_{12} &= \cos\psi \sin\phi + \sin\psi \cos\phi \cos\theta \\ h_{21} &= -\sin\psi \cos\phi - \cos\psi \sin\phi \cos\theta, & h_{22} &= \cos\psi \cos\phi - \sin\psi \sin\phi \cos\theta \\ h_{13} &= -\sin\theta \cos\phi, & h_{23} &= \sin\theta \sin\phi \\ h_{31} &= \sin\theta \cos\psi, & h_{32} &= \sin\theta \sin\psi, & h_{33} &= \cos\theta \end{aligned} \tag{9}$$

The constitutive relations

$$M_1 = d_1(\kappa_1 + \eta\dot{\kappa}_1), \qquad M_2 = d_2(\kappa_2 + \eta\dot{\kappa}_2), \qquad M_3 = d_3(\kappa_3 + \nu\dot{\kappa}_3) \tag{10}$$

where $d_k = D_k/D_2$ $(k = 1, 2, 3)$, $D_2 \geqslant D_1$ are the bending rigidities, D_3 is the torsional rigidity of a beam with solid cross section and η, ν are coefficients in the viscoelastic material relations $\sigma = E(\varepsilon + \eta\dot{\varepsilon})$, $\tau = G(\gamma + \nu\dot{\gamma})$. The similar relations were used in Nemat-Nasser and Tsai (1969) for the case of axial eccentric load.

3. Equilibrium of the plane bending of an uniform beam

Consider a beam loaded in the plane of its greatest rigidity by a follower force P (Fig. 1). In the pre-buckling configuration it can be assumed

$$F_2 = M_1 = M_3 = \kappa_1 = \kappa_3 = y = \phi = \psi = J = \dot{\kappa}_1 = \dot{\kappa}_3 = 0 \tag{11}$$

Eqs. (2), (4) and (6) are satisfied and Eqs. (1), (3), (5), (7) and (10) yield

$$F_1' + \kappa_2 F_3 = 0, \qquad F_3' - \kappa_2 F_1 = 0, \qquad M_2' + F_1 = 0, \qquad \kappa_2 = \theta', \qquad M_2 = \kappa_2 \tag{12}$$

From Eq. (12) one easily finds

$$F_1 = -\kappa_2', \qquad F_3 = C - \kappa_2^2/2 \tag{13}$$

where C is an integration constant and the curvature is to be found from nonlinear equation

$$\kappa_2' - C\kappa_2 + \frac{1}{2}\kappa_2^3 = 0 \tag{14}$$

The solution of Eq. (14) is taken as

$$\kappa_2 = A\frac{\mathrm{sn}(hs)}{\mathrm{dn}(hs)}, \qquad \kappa_2' = hA\frac{\mathrm{cn}(hs)}{\mathrm{dn}^2(hs)}$$
$$C = (2k^2-1)h^2, \qquad A^2 = 4k^2(1-k^2)h^2 \tag{15}$$

where $\mathrm{sn}(x,k)$, $\mathrm{cn}(x,k)$, $\mathrm{dn}(x,k)$ are Jacoby elliptic functions of modulus k. The boundary conditions at the loaded end $F_3(0) = M_2(0) = 0$, $F_1(0) = p$ yield

$$k^2 = 1/2, \qquad h^2 = p \tag{16}$$

From Eqs. (8) and (9) one finds

$$x' = \sin\theta, \qquad z' = \cos\theta, \qquad y' = 0$$
$$h_{12} = h_{21} = h_{23} = h_{32} = 0, \qquad h_{22} = 1, \qquad h_{31} = -h_{13} = \sin\theta, \qquad h_{33} = h_{11} = \cos\theta \tag{17}$$

and hence

$$J_2 = -\ddot{y}, \qquad J_1 = -(\ddot{x}\cos\theta - \ddot{z}\sin\theta), \qquad J_3 = -(\ddot{x}\sin\theta + \ddot{z}\cos\theta)$$

Using the boundary conditions at the clamped end $\theta(1) = x(1) = z(1) = 0$ the rotation and displacements can be calculated

$$\theta(s) = \int_s^1 \kappa_2(s) = 2\mathrm{arc\ tan}\,[\mathrm{cn}(h)] - 2\mathrm{arc\ tan}\,[\mathrm{cn}(hs)]$$
$$x(s) = \int_s^1 \sin\theta(s)\,\mathrm{d}s, \qquad z(s) = \int_s^1 [\cos\theta(s) - 1]\,\mathrm{d}s \tag{18}$$

4. Perturbed equations

Let for each variable

$$Z(s,t) = Z_0(s) + Z_p(s,t)$$

where $Z_0(s)$ is the value of the variable from Section 3, and $Z_p(s,t)$ is small perturbation. Insert this in Eqs. (1)–(10), neglect terms, nonlinear in perturbations and let

$$Z_p(s,t) = Z(s)\exp(qt) \tag{19}$$

The perturbed equations decouple in two groups.

Equations of bending in the plane of the greatest rigidity are

$$F_1' + \kappa_{20}F_3 + F_{30}\kappa_2 - q(X\cos\theta_0 - Z\sin\theta_0) = 0$$
$$F_3' - \kappa_{20}F_1 - F_{10}\kappa_2 - q(X\sin\theta_0 + Z\cos\theta_0) = 0$$
$$d_2(1+\eta q)\kappa_2' + F_1 = 0, \quad X - qx = 0, \quad Z - qz = 0$$
$$x' - \theta\cos\theta_0 = 0, \quad z' + \theta\sin\theta_0 = 0, \quad \theta' - \kappa_2 = 0 \tag{20}$$

and equations of flexure–torsion out of this plane

$$
\begin{aligned}
&F_2' + F_{10}\kappa_3 - F_{30}\kappa_1 - qY - \mu q y = 0\\
&d_1(1+\eta q)\kappa_1' - [1 - d_3(1+\nu q)]\kappa_{20}\kappa_3 - F_2 = 0\\
&d_3(1+\nu q)\kappa_3' + [1 - d_1(1+\eta q)]\kappa_{20}\kappa_1 = 0\\
&Y - qy = 0, \quad y' - \psi\sin\theta_0 = 0\\
&\psi'\sin\theta_0 - \theta_0'\phi + \kappa_1 = 0, \quad \psi'\cos\theta_0 + \phi' - \kappa_3 = 0
\end{aligned}
\tag{21}
$$

In Eqs. (20) and (21) the subscript 0 refers to the prebuckling configuration. The external friction force $\mu\dot{y}$ was added in the first Eq. (21).

5. Flexure–torsion problem

Eq. (21) is a system of ODE with variable coefficients and their analytic solution is not possible. The eigenvalue problem (21) with homogeneous boundary conditions

$$
F_2(0) = \kappa_1(0) = \kappa_3(0) = Y(1) = y(1) = \psi(1) = \phi(1) = 0 \tag{22}
$$

will be solved by the finite element method. Interval (0,1) is divided by points $s_i = i/N$, $i = 0, 1, \ldots, N$ into N equal elements and each variable is interpolated by a linear function

$$
\begin{aligned}
&Z(s) = N1(s)Z_i + N2(s)Z_{i+1}\\
&N1(s) = \frac{s_{i+1} - s}{\delta}, \quad N2(s) = \frac{s - s_i}{\delta}, \quad \delta = s_{i+1} - s_i = 1/N
\end{aligned}
\tag{23}
$$

Expression (23) is inserted into Eq. (21) and each Eq. (21) is integrated over the length of an element (subdomain collocation method). For instance, the first Eq. (21) after discretization becomes

$$
\begin{aligned}
&F_{2,i+1} - F_{2,i} - g2_i\kappa_{1,i+1} - g1_i\kappa_{1,i} + f2_i\kappa_{3,i+1} + f1_i\kappa_{3,i} - qn(Y_{i+1} + Y_i) - qn\mu(y_{i+1} + y_i) = 0\\
&g1_i = \int F_{30}N1\,\mathrm{d}s, \quad g2_i = \int F_{30}N2\,\mathrm{d}s, \quad f1_i = \int F_{10}N1\,\mathrm{d}s, \quad f2_i = \int F_{10}N2\,\mathrm{d}s\\
&n = \int N1\,\mathrm{d}s = \int N2\,\mathrm{d}s = \delta/2
\end{aligned}
\tag{24}
$$

where all integrals are from s_i to s_{i+1}.

For each element the discrete system is written in a matrix form

$$
AS_iU_i + AE_iU_{i+1} - q[BS_iU_i + BE_iU_{i+1}] = 0, \quad i = 0, 1, \ldots, N \tag{25}
$$

where the vector-column

$$
U_i = (F_{2,i}, K_{1,i}, K_{3,i}, Y_i, y_i, \psi_i, \phi_i)^{\mathrm{T}} \tag{26}
$$

The seven order matrix for the end of an element has a form:

$$
AE_i = \begin{bmatrix}
1 & -g2_i & f2_i & 0 & 0 & 0 & 0\\
-n & d_1 & -(1-d_3)c2_i & 0 & 0 & 0 & 0\\
0 & (1-d_1)c2_i & d_3 & 0 & 0 & 0 & 0\\
0 & 0 & 0 & 1 & 0 & 0 & 0\\
0 & 0 & 0 & 0 & 1 & -S2_i & 0\\
0 & n & 0 & 0 & 0 & S_i & -c2_i\\
0 & 0 & -n & 0 & 0 & C_i & 1
\end{bmatrix}
\tag{27}
$$

$$c2_i = \int \kappa_{20} N2 \, \mathrm{d}s, \qquad S2_i = \int N2 \sin\theta_0 \, \mathrm{d}s$$

$$S_i = \delta^{-1} \int \sin\theta_0 \, \mathrm{d}s, \qquad C_i = \delta^{-1} \int \cos\theta_0 \, \mathrm{d}s$$

Nonzero elements of the matrix BE_i are:

$$b_{14} = n, \quad b_{15} = n\mu, \quad b_{22} = -\eta d_1, \quad b_{23} = -\nu d_3 c2_i, \quad b_{32} = \eta d_1 c2_i, \quad b_{33} = -\nu d_3, \quad b_{45} = 1.$$

Matrix AS_i for the start of an element is obtained from Eq. (27) replacing C_i by $-C_i$, and changing sign of all diagonal elements. The sign of diagonal elements of BS_i also must be changed. Besides, values $g2, f2, c2, S2$ are replaced by $g1, f1, c2, S1$ which, in turn, are obtained replacing $N2$ by $N1$.

The eigenvalues equation is

$$\det(A - qB) = 0 \tag{28}$$

where system matrix A is assembled from element matrices as follows:

$$A = \begin{bmatrix} as_0 & AE_0 & A0 & A0 & c0 \\ a0 & AS_1 & AE_1 & A0 & c0 \\ a0 & A0 & AS_2 & AE_2 & c0 \\ a0 & A0 & A0 & AS_3 & ae_3 \end{bmatrix} \tag{29}$$

Here matrices as_0, ae_3 reflect the boundary conditions and are obtained from matrices AS_0, AE_3 respectively by deleting the appropriate columns. For instance, on the free end $F_2(0) = \kappa_1(0) = \kappa_3(0) = 0$ and columns number 1–3 in AS_0 must be deleted to obtain as_0. On the clamped end $Y(1) = y(1) = \psi(1) = \phi(1) = 0$ and to obtain ae_3 columns 4–7 must be deleted in AE_3. Zero matrix $A0$ is of the seventh order; zero matrix $a0$ have the same number of columns as as_0; zero matrix $c0$ have the same number of columns as ae_3. The same rules apply to matrix B.

Formula (29) is written for four elements but it clearly shows the simple assemble procedure for any number of them.

6. Numerical results

Calculations were performed with 20 elements for the beam with a rectangular cross-section (Fig. 1).

6.1. Undamped analysis

For a width–height ratio $b/h = 0.6$ the two lowest eigenvalues squared vs. dimensionless load

$$p = \frac{PL^2}{\sqrt{D_1 D_3}}$$

are shown in Fig. 2. As usually for problems with follower force, at some load ($p_c = 7.44$ in Fig. 2) the two dominant eigenvalues squared become equal. When the load is further increased, a pair of complex conjugate eigenvalues squared appear. Hence, one eigenvalue has a small positive real part and for $p > p_c = 7.44$ the system is unstable.

For $b/h = 0.7$ (Fig. 3) the picture is topologically different: the second eigenvalue increases with load and both lowest eigenvalues squared remain negative. Based on this two eigenvalues only, one may conclude that there is no critical load. However, at the load $p = p_c = 8.53943$ a large positive eigenvalue squared

emerges at the very end of the spectrum (spectrum is arranged in the order of an increased absolute value of eigenvalues). This critical (positive) eigenvalue q_N (where N is an ordinal number) is very sensitive to the load, as demonstrated in the table below.

P	q_N	N
8.53943	133000	16
8.53944	23300	14
8.53948	8250	13
8.53970	2680	11
8.54	1620	10
8.55	219	5

When the load is further increased, the positive eigenvalue reaches a minimum and then increases again.

Since for $N > 16$ (with 20 elements) all eigenvalues squared are infinite, one can say that the critical eigenvalue squared changes the sign from minus to plus at infinity.

The switch from Fig. 2 to Fig. 3-type takes place at $b/h \approx 0.65$. The important dissimilarity between these two types of instability is that for $b/h < 0.65$ the positive real part of critical eigenvalue near the boundary of instability is very small, while otherwise it is very large. This must affect the initial vibrations.

The critical loads, calculated with no damping, are shown in Fig. 4, curve 1. This curve shows that for $b/h \to 0$ (no prebuckling deformations), the critical load $p_c = 6.16$ as compared to $p_c = 6.99$ in Como (1966) for a concentrated mass, and $p_c \approx 6$ in Attard and Somervaille (1987).

Note, that the in-plane follower critical load for a cantilever beam is $PL^2/D_2 = 39$ (Vitaliani et al., 1997). For $b/h = 0.8$ this yields $p = PL^2/\sqrt{D_1 D_3} = 68.6$, so that even for a beam with almost quadratic cross-section the lateral critical load, Fig. 4, is much lower than the in-plane one.

When the load $p < p_c$ an undamped analysis yields all pure imaginary eigenvalues. In accordance with Liapunov theory, in this case the linearized perturbed equations (21) cannot serve to establish the stability or instability of the equilibrium. One way to clarify the situation is to include in the analysis damping, which produces nonzero real parts in the eigenvalues. The effect of both internal and external damping is considered in the next subsection.

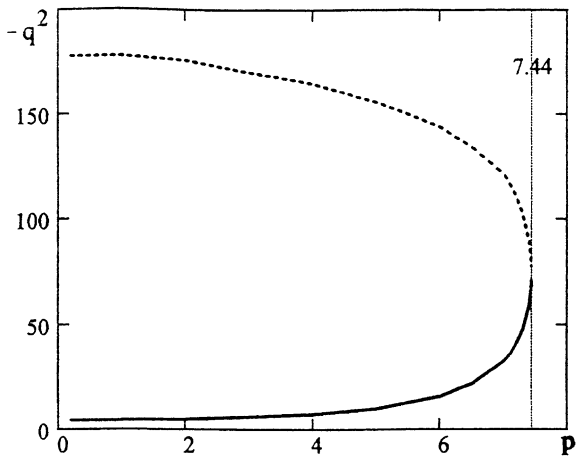

Fig. 2. Two lowest eigenvalues squared for $b/h = 0.6$. No damping.

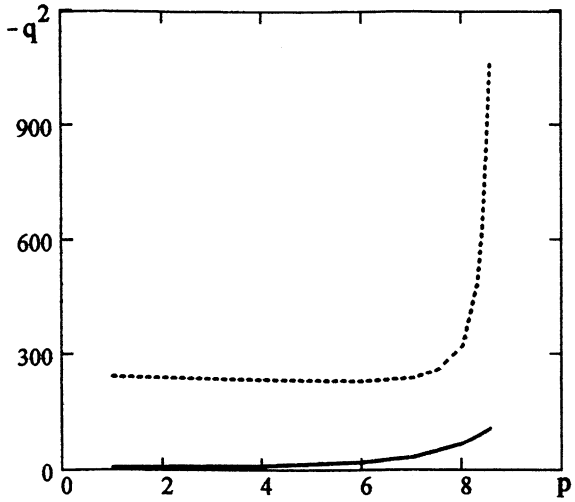

Fig. 3. Two lowest eigenvalues squared for $b/h = 0.7$. No damping.

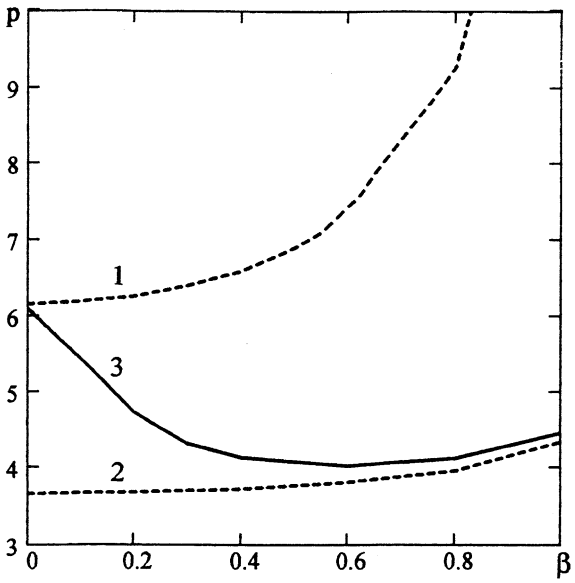

Fig. 4. Follower critical load vs. $\beta = b/h$: (1) no damping; (2) equal coefficients of internal damping for the normal and shear stress, $\eta = \nu = 0.001$. Coefficient of external damping $\mu = 0$; (3) $\eta = \nu = \mu = 0.001$.

6.2. Damped analysis

For the famous Beck problem (a column under axial follower load) the critical load decreases from 20.0 with no damping to 10.9 with a slight internal damping. When the external damping is added, the critical load approaches the value 20.0 (see Denisov and Novikov, 1975; Langhtjem and Sugiyama, 2000).

For the problem under consideration the effect of damping on the critical load is shown in Fig. 4. Curve 2 represents the effect of internal damping alone when coefficients of damping for normal and shear stress

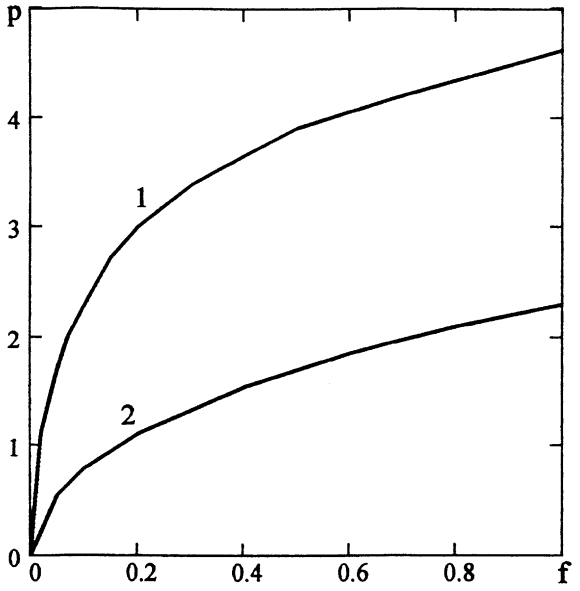

Fig. 5. Follower critical load versus external damping $\mu = vf$. (1) $b/h = 0.2$; (2) $b/h = 0.7$. Coefficients of internal damping: for the normal stress $\eta = 0$, for the shear stress $v = 0.001$.

are equal, $\eta = v = 0.001$. The stabilizing effect of the external damping (curve 3) is significant for a narrow rectangular but diminishes for a quadratic cross-section.

Destabilizing effect of the internal damping is even more significant for $\eta \to 0$, $v \neq 0$: the critical load in this case tends to zero (Fig. 5). When the external damping is increased, the critical load grows and for $\mu \geqslant 1$ exceeds the value, calculated with no damping. With any damping the critical eigenvalues are always the two lowest.

7. Conclusion

The lateral stability analysis of a beam under follower load should include slight internal and realistic external damping. With no damping the critical load will be overestimated. If the two principal rigidities of a beam are not far apart (ratio is higher than 0.42), and only two lowest eigenvalues are extracted, the wrong conclusion can be made that there is no finite critical load.

References

Attard, M.M., Somervaille, I.J., 1987. Stability of thin-walled open beams under nonconservative loads. Mech. Struct. Mach. 15, 395–412.

Barsoum, R.S., 1971. Finite element method applied to the problem of stability of a nonconservative system. Int. J. Num. Mech. Engng. 3, 63–87.

Bolotin, V.V., 1963. Nonconservative Problems of the Theory of Elastic Stability. Pergamon Press, Oxford.

Como, M., 1966. Lateral buckling of a cantilever subjected to a transverse follower force. Int. J. Sol. Struct. 2, 515–523.

Denisov G.G., Novikov V.V., 1975. On the stability of a rod under follower force. Mekhanika Tverdogo Tela 1, 150–154 (in Russian).

Detinko, F.M., 2000. On the elastic stability of uniform beams and circular arches under nonconservative loading. Int. J. Sol. Struct. 37, 5505–5515.

Hodges, D.H., Peters, D.A., 1975. On the lateral buckling of uniform slender cantilever beams. Int. J. Sol. Struct. 11, 1269–1280.
Langhtjem, M.A., Sugiyama, Y., 2000. Optimum design of cantilevered columns under the combined action of conservative and nonconservative loads. Part II: The damped case. Comput. Struct. 74, 399–408.
Love, A.E.H., 1944. A Treatise on the Mathematical Theory of Elasticity. Dover, New York.
Nemat-Nasser, S., Tsai, P.F., 1969. Effect of warping on stability of a bar under eccentric follower force. Int. J. Sol. Struct. 5, 271–279.
Vitaliani, R.V., Gasparini, A.M., Saetta, A.V., 1997. Finite element solution of the stability problem for nonlinear undamped and damped systems under nonconservative loading. Int. J. Sol. Struct. 34, 2497–2516.